THE JOURNAL OF PHYSICAL CHEMISTRY A

pubs.acs.org/JPCA Article

Spontaneous Symmetry Breaking in Cyclo[18]Carbon

Zenner S. Pereira and Edison Z. da Silva*

Cite This: J. Phys. Chem. A 2020, 124, 1152−1157 Read Online

ACCESS | Metrics & More | Article Recommendations | Supporting Information

ABSTRACT: After the experimental evidence of polyynic as the stable form of cyclo[18]carbon, in the present paper, using ab initio electronic structure calculations, we show that this result is a symmetry breaking event, a consequence of the second-order Jahn−Teller effect. We show that the eigenfunctions associated with lowest unoccupied molecular orbitals (LUMO) and LUMO + 1, the excited states of this ring molecule, interact with the eigenfunctions associated with the ground state (occupied states), and this interaction stabilizes the less symmetric polyynic form of cyclo[18] carbon with D_{9h} symmetry, instead of the cumulenic form. The frontier state interactions are responsible for the distortions in the symmetry in the electronic structures, lowering the energy and making the polyynic form the stable one with alternating triple and single bonds.

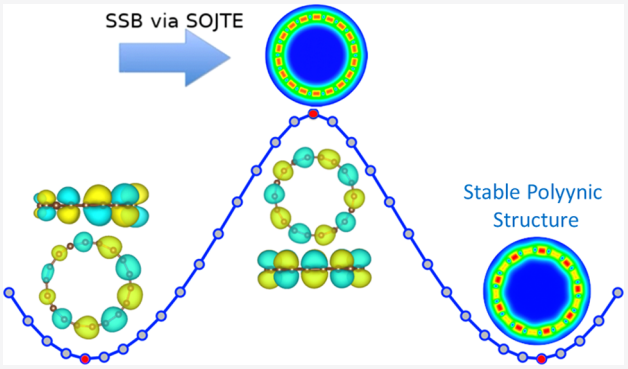

INTRODUCTION

Carbon, one of the most abundant elements in nature, fascinates by its ability to form many allotropes. Carbon atoms can form multiple covalent bonds with various other elements. This diversity brings innumerous possibilities to generate new structures or new compounds. Carbon allotropes can show diverse properties and can have very different applications. The classical example is graphite and diamond, while graphite is soft and is a conductor, diamond is one of the hardest structures known and is also an insulator. In the past decades, new carbon allotropes have been discovered, followed by new fields of basic research and applications. The examples are C_{60} fulerenes,[1] carbon nanotubes,[2] and graphene in this century.[3] Another carbon allotropic form is the long linear carbon chains[4] that are called cumulene (C) when formed by a sequence of double bonds, all with the same length, or named polyyne (P) type which has alternate short (triple bond) and long (single bond) bonds. Carbon also forms cyclic molecules with hydrogen, such as benzene (C_6H_6) or naphthalene ($C_{10}H_8$). When *n* carbon atoms form a cyclic closed chain, it is called cyclo[n]carbon, which can also have a polyyne or cumelene form.[5−8]

Recently, a joint research collaboration of IBM Research and Oxford University[9] presented experimental results of the production of cyclo[18]carbon (C_{18}) ring molecules. Using the STM/AFMA manipulation to strip oxygen from the precursor molecule $C_{24}O_6$, the ring molecule C_{18} was obtained. Characterization of the new structure using high-resolution AFM revealed a polyynic (P) structure, namely, a triple-bond and single-bond alternating structure with D_{9h} symmetry. Before this experiment, an intense theoretical debate occurred as to which was the more stable structure for the C_{18}. The results were divided in two groups, some favoring the cumulenic structure (C) with D_{18h} symmetry with equally spaced C atoms all shearing double bonds[10,11] and others favoring the polyynic structure (P) with D_{9h} symmetry with alternating triple (short) and single (long) bonds.[7,12] This divergence seems to have been resolved after the experimental work that observed the polyynic structure for cyclo[18]carbon. Recently, Baryshnikov[13] performed calculations that corroborated the polyynic structure for cyclo[18]carbon and showed that this result is not dependent on the substrate used in the experiment. The synthesis of C_{18} has opened the way to new research; many questions can be considered with respect to the interaction of this ring with other molecules[14] or other carbon allotropes or the interaction with other elements. The understanding of the electronic structure of this material is of fundamental importance in order to understand its properties as well as its interaction with other structures. We present here a detailed study of molecular and electronic structure of C_{18} that unfolds the quantum mechanical theoretical reasons for cyclo[18]carbon to prefer the polyynic form. This is a clear effect of spontaneous symmetry breaking (SSB),[15,16] where a highly symmetrical cumulene C_{18}, with group symmetry D_{18h}, suffers a distortion because of the second-order Jahn−Teller effect (SOJTE)[17−19] that changes

Received: December 21, 2019
Published: January 23, 2020

https://dx.doi.org/10.1021/acs.jpca.9b11822
J. Phys. Chem. A 2020, 124, 1152−1157

the equally spaced double-bond sequence (···C═C═C═C···) to the less symmetric triple (short) bond and single (long) bond (··· C≡C−CC≡C−C···), also changing the bond angles of adjacent bonds. This dimerization effect resembles a Peierls transition that occurs when the number of C atoms reaches infinity in the linear C chain.

Previous works have cited that SOJTE is responsible for the polyynic form of C_{18};[6−8] however, these works did not show the details of the J−T effect involved. Saito[8] presented a study of rings with $4N + 2$ atoms, where N is a natural number (N = 1, 2, 3...). For $N = 4$, which corresponds to the case C_{18}, the calculations have shown the cumulenic structure as the stable form. Another work by Torelli[7] indicates SOJTE as the reason for the polyynic structure found and explained it as the existence of a geometric dependence due to the electronic correlation of the system; although the analysis does not detail the J−T effect, it claims in a general way that there is a competition between conjugated aromaticity, SOTJE, and Peierls transition depending on the number of atoms in the ring.

METHODOLOGY

The electronic structure calculations of C_{18} were performed using the density functional theory (DFT) as implemented in the Quantum Espresso,[20,21] using hybrid exchange and correlation functional of the Perdew−Burke−Ernzerhof (PBE) type[22,23] with an exchange fraction of 0.8 instead of 0.25 as in a typical PBE0. A similar approach using exchange−correlation Heyd−Scuseria−Ernzerhof (HSE) hybrid functional[24] (with 0.8 exchange fraction) was presented by Kaiser et al. in their DFT calculations in order to obtain polyynic structure.[9] We used hybrid PBE functions with 0.8 mixing parameter in accordance with previous work by Atalla.[25] For this value of the exchange fraction in hybrid PBE, highest occupied molecular orbital (HOMO) and lowest unoccupied molecular orbitals (LUMO) functions show significant improvement in energy, and therefore, 0.8 appears to be a good choice for carbon atoms. As another example, in a letter published by Sai,[26] an exchange fraction of 0.7 was shown as a suitable choice for benzene. We also included the van der Walls correction of Tkatchenko−Sheffler.[27] The pseudopotential used was norm conserving (NC).[28] The kinetic energy cutoff used was 85 Ry for the wave functions, 340 Ry for the charge density, and 340 Ry for the exact exchange operator. The simulation box used was 22.23 × 22.23 × 18.90 Å, and the ring was relaxed with energy convergence with error smaller than 10^{-5} Ry and electronic density error less than 10^{-10} Ry. The strategy to search for the best structure followed a similar approach as previously described by Kaiser et al.[9]

PBE0 functionals, where part of the exchange correlation is calculated using the exact Hartree−Fock operator with an exchange fraction α, have been extensively used. The exchange correlation E_{xc} can be written as

$$E_{xc} = \alpha E_x^{Ex} + (1 - \alpha)E_x^{PBE} + E_c^{PBE} \quad (1)$$

where E_x^{PBE} and E_c^{PBE} are the exchange correlations as proposed by PBE[22] and E_x^{Ex} is the exchange calculated via the Hartree−Fock operator. α varies between 0 and 1, and α = 0.25 is commonly used. On the other hand, as suggested by Atalla,[25] the interaction of the frontier states are better represented with a larger value of α and in the range around 0.8 for carbon molecules. Other works have also shown the importance of using large values of α.[26,29] In similar functionals to PBE0 such as the HSE, the importance of the use of larger values of α was also shown.[9,13,30]

To clearly evaluate the adequate cutoff energy, we tested different values, namely, 45, 70, 85 and 100 Ry. Results show good convergence with around 85 Ry, the value used in the calculations. We also use 340 Ry for the charge density and the same value for the exact exchange operator cutoffs.

RESULTS

The reason for the polyynic form of cyclo[18]carbon with symmetry D_{9h} is an SSB that is driven by the distortion due to SOJTE. This effect is directly linked with the interaction of the fundamental and the exited states. Under certain constrains, ground-state eigenfunctions can interact with excited-state eigenfunctions, distorting the structure toward a more stable state.[31,32] In general, SOJTE occurs in high symmetry structures because of the fact that the distorted structure with less symmetry is more stable. The symmetry is affected only if a gain of stability occurs in the polyatomic system. In a high symmetry configuration, the interaction of ground-state eigenfunctions and the excited states has to fulfill two conditions simultaneously: (i) the eigenfunctions have to be of the same symmetry to guarantee a finite interaction and (ii) if condition (i) is satisfied, it is also necessary that the energy gap between the interacting eigenfunctions should not be too large, which would reduce drastically the effect of the interaction gap. The energy gap can be high, and even in such cases, the SOJTE still occurs, and in some cases, it can be in the range 10−15 eV.[15,16] The distortions caused by the SOJTE localize the electrons in the new molecular orbital.[33] Our results show a clear connection of the SOJTE as the effect driving cyclo[18]carbon to the polyynic structure. In our interpretation, polyynic cyclo[18]carbon with D_{9h} symmetry can be viewed as a spontaneous distortion of the D_{18h} cumulenic structure.

The results are organized as follows:(i) in the subsection structural and orbital analysis, we present the stable form of cyclo[18]carbon, the distortions present in the molecular orbitals, and the effects on the symmetry breaking in the local density of states (LDOS). This analysis is done in the high symmetry point, the cumulenic structure, and in the lowest symmetry point, the polyynic structure. The energy barrier of the structures is discussed. (ii) In the subsection Electronic Levels, we analyze and discuss the changes in the excited electronic states due to the interaction with the ground state as a function of the appropriate reaction coordinate. In conclusion, we connect the Jahn−Teller effect to the alterations due to symmetry breaking in the carbon ring, both from the geometry point of view and the relation to its electronic structure.

Structural and Orbital Analysis. The final stable polyynic structure has small bonds equal to 1.205 Å and long bonds equal to 1.356 Å, very similar to the ones obtained by Kaiser et al. in their DFT calculations and also similar to those obtained by Diederich.[12] A detailed analysis of the C_{18} frontier orbitals reveals distortion in some orbitals taking the C_{18} molecule to a less symmetric structure than expected for a C ring. These distortions are explained by the interaction of the excited-state eigenfunctions with the ground-state eigenfunctions of the unstable cumulene structure, as described by the last term of the SOJTE (see eqs 1 and 2 in the Supporting Information). Figure 1 (top panel) shows the excited molecular orbitals

https://dx.doi.org/10.1021/acs.jpca.9b11822
J. Phys. Chem. A 2020, 124, 1152−1157

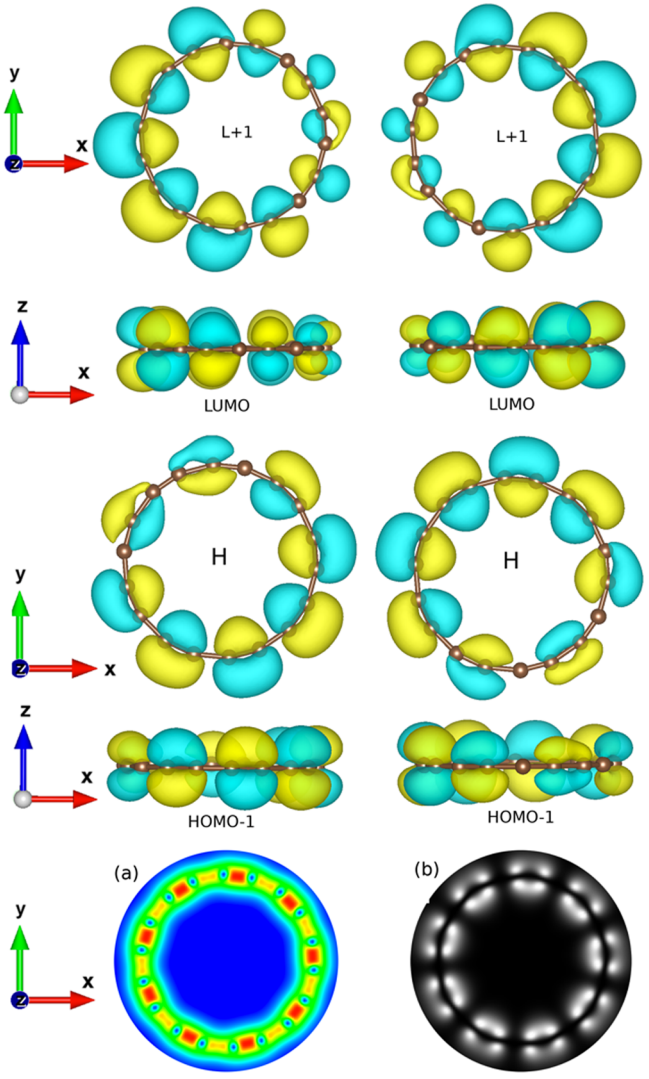

Figure 1. Top panel displays the LUMO (L). The picture shows two degenerate levels for each molecular orbital, LUMO and LUMO + 1, in different perspectives. The middle panel displays the HOMO and HOMO − 1. Colors represent the sign of the eigenfunction: green for positive values and yellow for negative values. The lower panel shows the simulated STM images of an STM tip at $z = 0$ height. (a) Color scale increases from blue indicating low LDOS to red indicating high LDOS. (b) Simulated STM result in gray scale. The bias volt is −3.9 eV below the Fermi level (−5.01 eV); white indicates high LDOS and black indicates low LDOS.

LUMO and LUMO + 1. LUMO + 1 is a twofold degenerate state formed by in-plane MOs at energy −1.12 eV, while LUMO is also a twofold degenerate state formed by MOs out of the C_{18} plane, with energy −1.15 eV. The wave functions of these excited states have 10 distributed nodes. Individually, they have lost part of their symmetry as displayed.

A plot similar to the LUMO and LUMO + 1 emerges in the case of HOMO and HOMO −1 MOs. The ground state also shows the result of the interaction with the excited states, caused by the SOJTE (eqs 1 and 2 in the Supporting Information). The HOMO and HOMO − 1 molecular orbitals are depicted in the middle panel of Figure 1. These are very similar to LUMO and LUMO + 1. The HOMO MOs are in plane while HOMO − 1 are orbitals perpendicular to the ring. The HOMO and HOMO − 1 orbitals show eight nodes. A detailed analysis shows that the interaction with the excited states involves deeper HOMOs going down to HOMO − 3; of course, the effect upon HOMO − 2 and HOMO − 3 is weaker because of the difference in energy from the excited states. For deeper states than HOMO − 3, the SOTJE is not significant. It is important to note that although the polyynic orbitals suffer distortions, reducing the number of symmetry axis, when the pair of orbitals is considered, the equilibrium of the probability density is restored. This can be seen when the LDOS is analyzed for the relevant energy range. The LDOS can be used to construct simulated STM images. Using the Tersoff and Hamann[34] formalism that gives the STM image, the tunneling current is proportional to the LDOS for an applied bias voltage, Figure 1a bottom panel, giving the resulting image formed due to the calculated electronic states. The image in the left is color-coded in blue for low intensity and red for high intensity. This image evidences clearly the nine sided polygon of the D_{9h} symmetry, it also shows with the high intensity triple (short bond, formed by two π and one σ bonds) bond in red and the single (long) one in yellow. This effect does not occur in the cumulenic structure (see Figure S1 in the Supporting Information). The HOMO orbital pair that lost part of its symmetry, when combined together in the LDOS, recovers its symmetry. Figure 1b shows the STM image with bias voltage adequate to show only the HOMO contribution. In fact, the total effect of distortions is related to the observed cyclo[18] carbon structure. The orbital distortions and changes in the energy of the electronic levels leads the way to the explanation of SOJTE as the cause to the polyynic structure of cyclo[18]carbon.

To confirm the interpretation that cyclo[18]carbon in the polyynic structure with D_{9h} symmetry is a distortion of the cumulenic D_{18h} structure, it is important to observe that the structural change between the structures is small. The change in bond length, from equal bonds in cumulene to short−long bonds in the polyynic form, is very small and less than 0.08 Å, which means that the reaction path from the C to the P structure is small and accompanied by a change in bond angles. These changes are very small when compared with the cyclo[18]carbon radius (approximately 3.7 Å). The polyynic structure can be obtained in a good approximation with small changes in the bond lengths of the cumulenic structure, which is equivalent to changing the angular coordinates Q_θ by changing the position of the atoms of the cumulenic structure. A similar procedure was used by Torelli[7] to determine the minimum energy of polyynic cyclo[18]carbon. Figure 2 shows the energy change that leads the C structure to transform to P due to SOJTE. Figure 2a shows the HOMO−LUMO MOs and the energy gap for both structures. The evolution from C to P increases the gap, as is usual in SOJTE-driven transformations. Taking the cumulenic structure without distortion ($Q_\theta = 0$), we calculated the total energy as a function of Q_θ shown in Figure 2b. The energy minimum is reached for the polyynic structure. It is clearly observed that the cumulenic structure is at an energy maximum with totally symmetric orbitals with no distortion. This is the perfect scenario for the SOJTE. Any small changes ($Q_\theta \neq 0$) trigger the SOJTE, driving the system to a new and more stable minimum. The arrows in Figure 2b indicate the high symmetry (D_{18h}) structure maximum C and the less symmetrical (D_{9h}) structure as the stable minima P (see also the video in the Supporting Information).

https://dx.doi.org/10.1021/acs.jpca.9b11822
J. Phys. Chem. A 2020, 124, 1152−1157

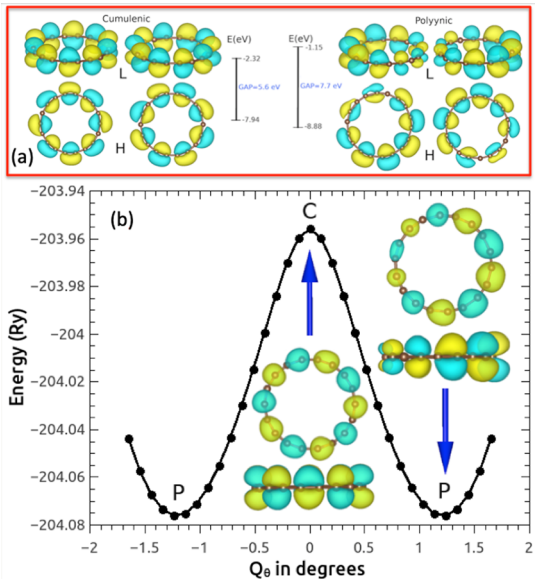

Figure 2. HOMO and LUMO MOs and total energy change. (a) Cumulenic and polyynic HOMO−LUMO and the gaps of both structures. (b) Total energy change as a function of the reaction coordinate Q_θ (each step is approximately 0.104°). The polyynic structure is obtained as a minimum after 12 steps. The points C and P are the unstable cumulenic and stable polyynic structures, respectively. The inset shows the LUMO for the structures C and P with two views each.

The energy difference between the cumulenic and polyynic structures obtained in the present calculations, employing PBE0 with NC pseudopotential, is 36.3 kcal/mol. This result is in good agreement with the coupled-cluster singles and doubles excitation theory calculations by Arulmozhiraja[6] who found the value of 32.11 kcal/mol and is also in agreement with a multiconfigurational self-consistent-field (MCSCF) calculation presented by Torelli and Mitas (36.8 kcal/mol).[7] Calculations by Nandi et al.[35] using canonical variational transition state theory and the small-curvature tunneling found an energy barrier of 40.2 kJ/mol (9.6 kcal/mol); this value is significantly smaller than the results using MCSCF as well as our present results. Nandi et al. concluded that carbon atoms can suffer automerization because of quantum tunneling having this cumulenic energy barrier.

Electronic Levels. We also investigated how the electronic states of the different orbitals evolve in energy as a function of the reaction coordinate due to the SOJTE. Table 1 shows a comparison of the frontier orbital energies for both C and P structures. It also shows that the number of nodes goes down as one moves to lower orbitals; these are always even numbers and go to zero. We note that the excited orbitals go up in energy and the ground state lowers as the structure evolves from C to P. As the excited state goes up and the ground state goes down, the HOMO−LUMO gap increases from 5.6 to 7.72 eV. Table 1 shows that HOMO and HOMO − 1 have a significant decrease in energy for the P structure. For HOMO − 2 and HOMO − 3, there is a small reduction, and for HOMO − 4 and HOMO − 5, the behavior is the opposite. Overall, there is an increased stability for the HOMO to HOMO − 3 in the P structure, but states below HOMO − 03 are more stable in the C structure. This drives a competition that finds a minimum away from the high symmetry in the polyynic structure for C_{18}.

Table 1. Energy Levels for Cumulenic and Polyynic Structures in eV Using PBE0 with NC Pseudopotential[a]

electronic level	nodes	cumulenic	polyynic
LUMO + 1	10	−2.279	−1.118
LUMO	10	−2.318	−1.153
HOMO	8	−7.94	−8.877
HOMO − 1	8	−8.084	−9.020
HOMO − 2	6	−11.364	−11.461
HOMO − 3	6	−11.458	−11.561
HOMO − 4	4	−13.625	−13.561
HOMO − 5	4	−13.663	−13.603

[a]The number of nodes is also presented.

We also performed similar calculations with projected augmented wave (PAW) pseudopotentials[36] using exchange−correlation HSE hybrid functional[24] with 0.8 as an exchange fraction. Those results have shown the same effects presented in this work, with the only difference occurring in the energy values of the orbitals. The HOMO−LUMO gap for HSE was 5.3 eV. This result is presented in Table 2.

Table 2. Energy Levels for Cumulenic and Polyynic Structures in eV Using HSE with PAW[a]

electronic level	nodes	cumulenic	polyynic
LUMO + 1	10	−3.267	−2.357
LUMO	10	−3.321	−2.406
HOMO	8	−7.000	−7.713
HOMO − 1	8	−7.142	−7.853
HOMO − 2	6	−10.160	−10.252
HOMO − 3	6	−10.254	−10.350
HOMO − 4	4	−12.372	−12.322
HOMO − 5	4	−12.415	−12.370

[a]The number of nodes is also presented.

Figure 3 shows (using PBE0 with NC pseudopotential) the changes in energy of the important energy levels because of the SOJTE as they evolve. This behavior is in agreement with the SOJTE equations (see the Supporting Information). When a ground-state eigenvalue is affected by the interaction with an excited state, the SOJTE parabolic term with downward concavity dominates, causing a decrease in the ground-state energy. This can be seen in Figure 3a for the case of HOMO and HOMO − 1 as a function of Q_θ. On the other hand, the excited states grow in energy as shown in Figure 3b for the LUMO and LUMO + 1 states (top panel). Therefore, the ground state gains stability at the expense of the excited state. One term tries to restore the high symmetry (second term with upward concavity) as the other term, which involves the interaction with the excited states which is always negative, reduces the energy. This competition results in the equilibration of the structure in a lower symmetry, the symmetry braking change from D_{18h} to D_{9h} due to the SOJTE. Figure 3c shows that the JTE interaction diminishes for the HOMO − 2 and HOMO − 3, at this stage, around the high symmetry $Q_\theta = 0$ point is possible to observe a strong competition between the positive and negative terms. The negative term responsible for the SOTJE wins when there is a small fluctuation around this point.

In the case of HOMO − 4 and HOMO − 5 (Figure 3d), we observe a parabolic behavior with upward concavity, which

https://dx.doi.org/10.1021/acs.jpca.9b11822
J. Phys. Chem. A 2020, 124, 1152−1157

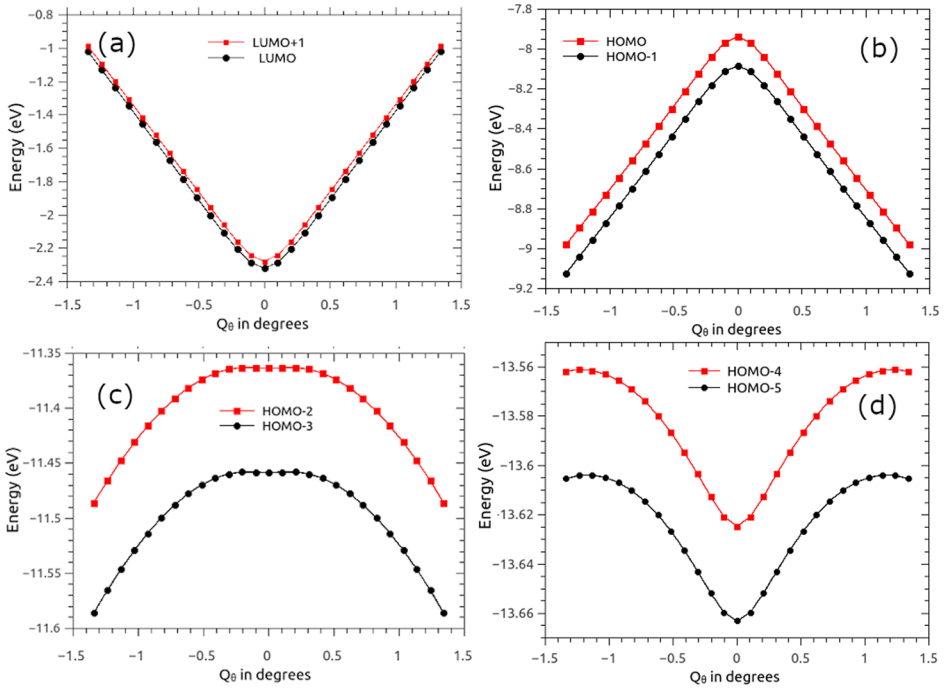

Figure 3. Changes in the electronic levels when the structure evolves with the reaction coordinate Q_θ, as in Figure 2, from P to C. (a) LUMO and LUMO + 1. (b) HOMO and HOMO − 1. (c) HOMO − 2 and HOMO − 3. (d) HOMO − 4 and HOMO − 5. The polyynic structure is obtained as a minimum after 12 steps.

shows that for these levels, the interaction with the excited states does not affect the cyclo[18]carbon geometry, which means that SOJTE goes down for the deeper levels. The interaction in the SOJTE occurs within states of the same symmetry; therefore, ground-state eigenfunctions with symmetry in the ring plane interact with excited-state eigenfunctions of the same symmetry (HOMO − 2, HOMO and LUMO + 1). In the same spirit, eigenfunctions with perpendicular symmetry to the ring interact with the similar symmetry excited states (HOMO − 3 and HOMO − 1 and LUMO). As a final note, we comment on the nature of the stable polyynic form of this carbon ring. As can be observed in Figure 2b, the energy profile has two degenerate minima which correspond to the reaction coordinate attaining positive (the case shown and discussed so far) and negative values. The meaning of this result is that if one considers one carbon atom in the cumulenic ring (···C═C═C···), the SOTJE can shorten and elongate its bonds in two ways, namely, (···C≡C−C···) or (···C−C≡C···) depending on Q_θ being positive or negative (see also Figure S4). These are the two degenerate forms in which cyclo[18]carbon can evolve to the stable polyynic form. These two structures resemble the Kekule resonating states seen in other ring structures.

CONCLUSIONS

In conclusion, using electronic ab initio calculations, this paper presented a clear explanation for the stability of the polyynic form of the recently experimentally obtained cyclo[18]carbon. The reason for the observed and simulated structure to be the stable one is a direct consequence of symmetry breaking, driven by the SOJTE. We have shown that the eigenfunctions of the excited states interact with the ground state, the depth of this interaction goes as far as HOMO − 3, with the consequence that the molecular orbitals of the unstable cumulenic structure undergoes changes, and these interactions lead to distortions that lower symmetry of cyclo[18]carbon according with SOJTE. Therefore, this theoretical problem that has been discussed since many decades finds a simple and clear solution in the light of SOJTE.

ASSOCIATED CONTENT

Supporting Information

The Supporting Information is available free of charge at https://pubs.acs.org/doi/10.1021/acs.jpca.9b11822.

SOJTE; STM images; and molecular orbitals (PDF)

Simple overview of the SOJTE in action for cyclo[18]-carbon (AVI)

AUTHOR INFORMATION

Corresponding Author

Edison Z. da Silva − *Institute of Physics "Gleb Wataghin", UNICAMP, CP 6165, 13083-9859 Campinas, São Paulo, Brazil;* orcid.org/0000-0002-2195-0051; Email: zacarias@ifi.unicamp.br

Author

Zenner S. Pereira − *Departamento de Ciência e Tecnologia, Universidade Federal Rural do Semi-Árido (UFERSA), 59780000 Caraúbas, Rio Grande do Norte, Brazil;* orcid.org/0000-0002-9253-6341

Complete contact information is available at: https://pubs.acs.org/10.1021/acs.jpca.9b11822

Author Contributions

The simulations were performed at the CCJR computers and CENAPAD-SP. The following agencies contributed funds for this research: CAPES—Finance code 001, PNPD Program, FINEP, FAPESP (2013/07296-2, 2016/23891-6), and CNPq (EZDS, 304073/2015-6)

Notes

The authors declare no competing financial interest.

REFERENCES

(1) Kroto, H. W.; Heath, J. R.; O'Brien, S. C.; Curl, R. F.; Smalley, R. E. C60: Buckminsterfullerene. *Nature* **1985**, *318*, 162−163.
(2) Iijima, S. Helical microtubules of graphitic carbon. *Nature* **1991**, *354*, 56−58.
(3) Novoselov, K. S.; Geim, A. K.; Morozov, S. V.; Jiang, D.; Zhang, Y.; Dubonos, S. V.; Grigorieva, I. V.; Firsov, A. A. Electric Field Effect in Atomically Thin Carbon Films. *Science* **2004**, *306*, 666−669.
(4) Shi, L.; Rohringer, P.; Suenaga, K.; Niimi, Y.; Kotakoski, J.; Meyer, J. C.; Peterlik, H.; Wanko, M.; Cahangirov, S.; Rubio, A.; Lapin, Z. J.; Novotny, L.; Ayala, P.; Pichler, T. Confined linear carbon chains as a route to bulk carbyne. *Nat. Mater.* **2016**, *15*, 634−639.
(5) Martin, J. M. L.; El-Yazal, J.; François, J.-P. Structure and vibrational spectra of carbon clusters Cn (n = 2−10, 12, 14, 16, 18) using density functional theory including exact exchange contributions. *Chem. Phys. Lett.* **1995**, *242*, 570−579.
(6) Arulmozhiraja, S.; Ohno, T. CCSD calculations on C14, C18, and C22 carbon clusters. *J. Chem. Phys.* **2008**, *128*, 114301.
(7) Torelli, T.; Mitas, L. Electron Correlation in C_{4N+2} Carbon Rings: Aromatic versus Dimerized Structures. *Phys. Rev. Lett.* **2000**, *85*, 1702−1705.
(8) Saito, M.; Okamoto, Y. Second-order Jahn-Teller effect on carbon 4N + 2 member ring clusters. *Phys. Rev. B: Condens. Matter Mater. Phys.* **1999**, *60*, 8939−8942.
(9) Kaiser, K.; Scriven, L. M.; Schulz, F.; Gawel, P.; Gross, L.; Anderson, H. L. An sp-hybridized molecular carbon allotrope, cyclo[18] carbon. *Science* **2019**, *365*, 1299−1301.
(10) Hoffmann, R. Extended hückel theory—v: Cumulenes, polyenes, polyacetylenes and cn. *Tetrahedron* **1966**, *22*, 521−538.
(11) Parasuk, V.; Almlof, J.; Feyereisen, M. W. The [18] all-carbon molecule: cumulene or polyacetylene? *J. Am. Chem. Soc.* **1991**, *113*, 1049−1050.
(12) Diederich, F.; Rubin, Y.; Knobler, C. B.; Whetten, R. L.; Schriver, K. E.; Houk, K. N.; Li, Y. All-Carbon Molecules: Evidence for the Generation of Cyclo[18] carbon from a Stable Organic Precursor. *Science* **1989**, *245*, 1088−1090.
(13) Baryshnikov, G. V.; Valiev, R. R.; Kuklin, A. V.; Sundholm, D.; Ågren, H. Cyclo[18] carbon: Insight into Electronic Structure, Aromaticity, and Surface Coupling. *J. Phys. Chem. Lett.* **2019**, *10*, 6701−6705.
(14) Maier, S. An atomic-scale view of cyclocarbon synthesis. *Science* **2019**, *365*, 1245−1246.
(15) Bersuker, I. B.; Gorinchoi, N. N.; Polinger, V. Z. On the origin of dynamic instability of molecular systems. *Theor. Chim. Acta* **1984**, *66*, 161−172.
(16) Bersuker, I. B. Pseudo-Jahn−Teller Effect—A Two-State Paradigm in Formation, Deformation, and Transformation of Molecular Systems and Solids. *Chem. Rev.* **2013**, *113*, 1351−1390.
(17) Jahn, H. A.; Teller, E.; George, D. F. Stability of polyatomic molecules in degenerate electronic states - I—Orbital degeneracy. *Proc. R. Soc. A* **1937**, *161*, 220−235.
(18) Pearson, R. G. The second-order Jahn-Teller effect. *J. Mol. Struct.: THEOCHEM* **1983**, *103*, 25−34.
(19) Pearson, R. G. Concerning Jahn-Teller Effects. *Proc. Natl. Acad. Sci. U.S.A.* **1975**, *72*, 2104−2106.
(20) Giannozzi, P.; Baroni, S.; Bonini, N.; Calandra, M.; Car, R.; Cavazzoni, C.; Ceresoli, D.; Chiarotti, G. L.; Cococcioni, M.; Dabo, I.; et al. QUANTUM ESPRESSO: a modular and open-source software project for quantum simulations of materials. *J. Phys.: Condens. Matter* **2009**, *21*, 395502.
(21) Giannozzi, P.; Andreussi, O.; Brumme, T.; Bunau, O.; Buongiorno Nardelli, M.; Calandra, M.; Car, R.; Cavazzoni, C.; Ceresoli, D.; Cococcioni, M.; et al. Advanced capabilities for materials modelling with Quantum ESPRESSO. *J. Phys.: Condens. Matter* **2017**, *29*, 465901.
(22) Perdew, J. P.; Burke, K.; Ernzerhof, M. Generalized Gradient Approximation Made Simple. *Phys. Rev. Lett.* **1996**, *77*, 3865−3868.
(23) Adamo, C.; Barone, V. Toward reliable density functional methods without adjustable parameters: The PBE0 model. *J. Chem. Phys.* **1999**, *110*, 6158−6170.
(24) Heyd, J.; Scuseria, G. E.; Ernzerhof, M. Hybrid functionals based on a screened Coulomb potential. *J. Chem. Phys.* **2003**, *118*, 8207−8215.
(25) Atalla, V.; Yoon, M.; Caruso, F.; Rinke, P.; Scheffler, M. Hybrid density functional theory meets quasiparticle calculations: A consistent electronic structure approach. *Phys. Rev. B: Condens. Matter Mater. Phys.* **2013**, *88*, 165122.
(26) Sai, N.; Barbara, P. F.; Leung, K. Hole Localization in Molecular Crystals from Hybrid Density Functional Theory. *Phys. Rev. Lett.* **2011**, *106*, 226403.
(27) Tkatchenko, A.; Scheffler, M. Accurate Molecular Van Der Waals Interactions from Ground-State Electron Density and Free-Atom Reference Data. *Phys. Rev. Lett.* **2009**, *102*, 073005.
(28) Hamann, D. R. Optimized norm-conserving Vanderbilt pseudopotentials. *Phys. Rev. B: Condens. Matter Mater. Phys.* **2013**, *88*, 085117.
(29) Lau, V. W.-h.; Moudrakovski, I.; Botari, T.; Weinberger, S.; Mesch, M. B.; Duppel, V.; Senker, J.; Blum, V.; Lotsch, B. V. Rational design of carbon nitride photocatalysts by identification of cyanamide defects as catalytically relevant sites. *Nat. Commun.* **2016**, *7*, 12165.
(30) Patera, L. L.; Queck, F.; Scheuerer, P.; Moll, N.; Repp, J. Accessing a Charged Intermediate State Involved in the Excitation of Single Molecules. *Phys. Rev. Lett.* **2019**, *123*, 016001.
(31) Wedler, H. B.; Wendelboe, P.; Power, P. P. Second-Order Jahn−Teller (SOJT) Structural Distortions in Multiply Bonded Higher Main Group Compounds. *Organometallics* **2018**, *37*, 2929−2936.
(32) Silvestre, J.; Tremel, W.; Hoffmann, R. A second-order Jahn-Teller distortion in the solid: the phase transition in VSx. *J. Less-Common Met.* **1986**, *116*, 113−128.
(33) Kutzelnigg, W. The Molecular Orbital Theory of Conjugated Systems. *Angew. Chem.* **1967**, *79*, 486−491.
(34) Tersoff, J.; Hamann, D. R. Theory of the scanning tunneling microscope. *Phys. Rev. B: Condens. Matter Mater. Phys.* **1985**, *31*, 805−813.
(35) Nandi, A.; Solel, E.; Kozuch, S. Carbon Tunneling in the Automerization of Cyclo[18] carbon. *Chem.—Eur. J.* **2019**, *26*, 625.
(36) Blöchl, P. E. Projector augmented-wave method. *Phys. Rev. B: Condens. Matter Mater. Phys.* **1994**, *50*, 17953−17979.

https://dx.doi.org/10.1021/acs.jpca.9b11822
J. Phys. Chem. A 2020, 124, 1152−1157